RSC Advances

PAPER

View Article Online
View Journal | View Issue

Cite this: *RSC Adv.*, 2017, **7**, 50875

Isolation, structure elucidation, and KDD study of (−)-Celosine, a new skeleton with potent anti-atherosclerosis activity†

Zhenliang Sun,[ac] Zhiliang Lv,[*b] Bin Hu,[d] Jifa Zhang,[a] Peng Du,[b] Man Wang,[a] Linlin Xiao[a] and Peiming Yang[*c]

Received 6th August 2017
Accepted 25th October 2017

DOI: 10.1039/c7ra08683k

rsc.li/rsc-advances

Natural (−)-Celosine was isolated as a novel endocyclicditerpene with an unprecedented skeleton from *Celosia cristata* L. Its structure was established by comprehensive 1D and 2D NMR spectroscopic analysis in combination with single-crystal X-ray crystallographic diffraction of synthesized (+)-Celosine. (−)-Celosine was expected to have an anti-atherosclerotic activity *in vivo*, and myeloperoxidase (MPO) expression may be the mechanism underlying this anti-atherosclerotic activity.

Introduction

Celosia cristata L., known as Jiguanhua *etc.* in Chinese, has been long used in traditional Chinese medicine (TCM) for the treatment of hematischesis, infection, and hypertension.[1–4] Previous studies[5–7] on the whole dry plant of *Celosia cristata* L. have led to the isolation of many structurally novel compounds. The diversity of these novel compounds from *Celosia cristata* L. encouraged chemists to dig deep for new compounds, especially with a novel skeleton. In the present study, we selected *Celosia cristata* L. as the subject of our research and made a further investigation on their chemical constituents and pharmacological activities. By using various separation methods and chromatographic techniques, a chalcone–monoterpene complex was isolated, which represented a novel carbon skeleton of a natural endocyclic compound possessing 5 chiral centers (Fig. 1). This novel endocyclic skeleton was first obtained from natural source *C. cristata* of *Celosia* and named as "Celosine".

Results and discussion

Celosine was obtained as a white amorphous powder. The HR-ESI-MS showed a quasi-molecular ion peak at *m*/*z* 437.2314 $[M+H]^+$ (calcd for $C_{27}H_{33}O_5$, 437.2328), suggesting a molecular formula $C_{27}H_{32}O_5$ with 12 double-bond equivalents (DBEs). The IR spectrum displayed absorptions for hydroxyls (3394 cm^{-1}) and double bonds (1622 and 1589 cm^{-1}). The ^1H NMR spectrum (Table 1) showed typical signals of one hydrogen-bonded hydroxyl group at δ_H 14.22 (s), six aromatic protons, one olefinic proton at δ_H 5.49 (1H, br. d, J = 6.4 Hz), two methoxyl groups (δ_H 3.90, 3.87, each 3H, s) and three methyl groups at δ_H 1.93 (3H, d, J = 1.7 Hz), 0.90 (3H, d, J = 6.6 Hz) and 0.84 (3H, d, J = 6.5 Hz). The five typical signals at δ_H 7.29 (2H, m), 7.26 (2H, m), 7.18 (1H, br. t, J = 7.2 Hz) indicated the presence of mono-substituted benzene while the remaining single aromatic proton signal at δ_H 6.03 (1H, s) indicated a penta-substituted benzene. The ^{13}C NMR and DEPT spectra data (Table 1), with the aid of HSQC experiments, further revealed the presence of one mono-substituted benzene, one penta-substituted benzene, one double bond, one carbonyl, three methyl groups, two methoxyl groups, one sp^3 methylene and six sp^3 methines. The proton resonance at δ_H 14.22 showed no correlation with any carbons in the HSQC spectrum and were assigned to the hydroxyl. The above-mentioned functionalities accounted for 10 DBEs, and the remaining 2 DBEs require the existence of 2 additional rings in the molecule.

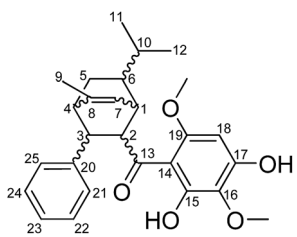

(-)-Celosine **(1)**

Fig. 1 2D structure of (−)-Celosine (**1**).

[a]*6th People's Hospital South Campus, Shanghai Jiao Tong University, Shanghai, China*
[b]*Zhangjiang Branch Institute of Chinese State Institute of Pharmaceutical Industry, Shanghai, China*
[c]*State Key Laboratory of New Drug and Pharmaceutical Process, Shanghai Institute of Pharmaceutical Industry, China State Institute of Pharmaceutical Industry, Shanghai, China*
[d]*Instrumental Analysis Center, Chinese State Institute of Pharmaceutical Industry, Shanghai, China*

† Electronic supplementary information (ESI) available: Experimental procedures, product characterizations, and ^1H and ^{13}C NMR spectra. CCDC 1488037. For ESI and crystallographic data in CIF or other electronic format see DOI: 10.1039/c7ra08683k

Table 1 The ^{1}H, ^{13}C NMR data of (−)-Celosine (**1**) ($CDCl_3$; δ, ppm; J, Hz)

No.	δ_H (J in Hz)	δ_C	DEPT
1	2.97 d (6.4)	39.0	CH
2	4.09 dd (6.8, 1.5)	56.2	CH
3	3.61 br. d (7.1)	42.6	CH
4	2.45 t (2.3)	43.4	CH
5α	1.92 (overlapped)	25.8	CH_2
5β	0.78–0.82 (overlapped)		
6	1.52 tdd (9.5, 4.7, 2.0)	49.0	CH
7	5.49 br. d (6.4)	120.0	CH
8	—	145.8	C
9	1.93 d (1.7)	19.9	CH_3
10	1.14 dp (9.4, 6.4)	33.4	CH
11	0.90 d (6)	21.3	CH_3
12	0.84 d (6.5)	20.8	CH_3
13	—	206.2	C
14	—	105.6	C
15	—	159.1	C
16	—	128.6	C
17	—	154.6	C
18	6.03 s	89.3	CH
19	—	158.5	C
20	—	143.8	C
21	7.26 (overlapped)	128.1	CH_2
22	7.29 (overlapped)	128.3	CH_2
23	7.18 br. t (7.2)	125.9	CH_2
24	7.29 (overlapped)	128.3	CH_2
25	7.26 (overlapped)	128.1	CH_2
15-OH	14.22 s	—	—
16-OCH_3	3.87 s	16.5	CH_3
19-OCH_3	3.90 s	17.5	CH_3

The planar structure of Celosine was established by interpretation of 2D NMR spectra (^{1}H–^{1}H COSY, HSQC and HMBC). The ^{1}H–^{1}H COSY spectrum (Fig. 2) displayed four coupled spin systems of H-1 (δ_H 2.97)/H-2 (δ_H 4.09)/H-3 (δ_H 3.61)/H-4 (δ_H 2.45)/H-5 (δ_H 1.92, 0.80)/H-6 (δ_H 1.52)/H-1 (δ_H 2.97); H-1 (δ_H 2.97)/H-7 (δ_H 5.49); H-6 (δ_H 1.52)/H-10 (δ_H 1.14)/H-11 (δ_H 0.90) (/H-12 (δ_H 0.84)) and H-21 or 25 (δ_H 7.26)/H-22 or 24 (δ_H 7.29)/H-23 (δ_H 7.18). The coupled spin systems from H-1 to H-6 indicated the existence of a ring with six carbons.

The downfield chemical shift of hydroxyl (δ_H 14.22) suggested its double-bonding position (thus adjacent) to the carbonyl group. The multiple HMBC correlations (Fig. 3) of 15-OH/C-14 and C-16; H-16/C-16; H-18/C-13, C-14, C-16, C-17 and C-19; 19-OCH_3/C-19 established the 2,4-dihydroxy-3,6-dimethoxybenzoyl group. The HMBC correlations of H-2/C-20, H-3/C-21, H-21/C-3 suggested the location of mono-substituted benzyl moiety at C-3. The HMBC correlations of H-11/C-6, H-11/C-12, H-1/C-10, H-2/C-6 together with ^{1}H–^{1}H COSY correlations of H-6/H-10/H-11(H-12) revealed the presence of the isopropyl at C-6. The HMBC correlations of H-18/C-13, H-1/C-13, H-2/C-13 suggested the location of carbonyl group at C-2 and C-14. After counting the above six membered ring as one DBEs, the last DBE in the molecule was solved by revealing the double bond bridge between C-1 and C-4 forming a second ring with the HMBC correlations of H-1/C-8, H-2/C-7, H-4/C-7 and ^{1}H–^{1}H COSY correlation of H-1/H-7. The HMBC correlations of H-4/C-9 and H-9/C-7 indicated a methyl locating at C-8 position. The planar structure of Celosine was thus established.

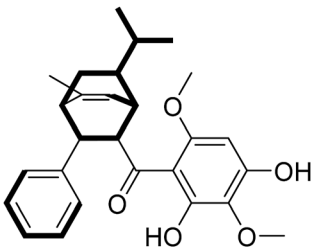

Fig. 2 Key ^{1}H–^{1}H COSY correlations (bold bonds) of (−)-Celosine.

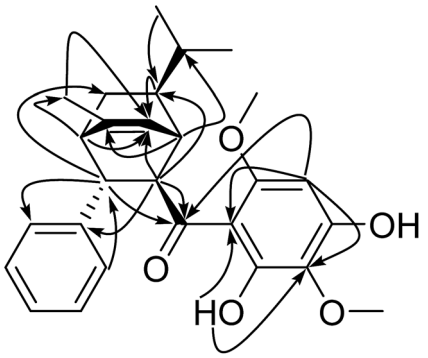

Fig. 3 Key HMBC correlations (arrows) of (−)-Celosine.

The relative configuration of Celosine was assigned by ROESY (Fig. 4) spectrum. The correlations of H-5α with H-1, H-2 and H-2 with H-4, H-6 revealed that H-1, H-2, H-4, H-5α and H-6 were cofacial and randomly assigned to be α-oriented. The correlations of 9-CH_3 with H-5β and H-3 revealed that H-5β, H-3 and 9-CH_3 were cofacial and β-oriented. The two possible configurations were shown in Fig. 5.

Mp 59.5–60.2 °C, IR (KBr) V_{max}: 3394, 1621, 1589 and 1427 cm^{-1}, $[\alpha]_D^{25} = -139.4$ ($c = 0.1$, MeOH). The suitable single-crystal could not be obtained from the natural source of Celosine due to the less amount of the sample. Therefore, the total synthesis of Celosine was carried out to determine the absolute configuration of Celosine.

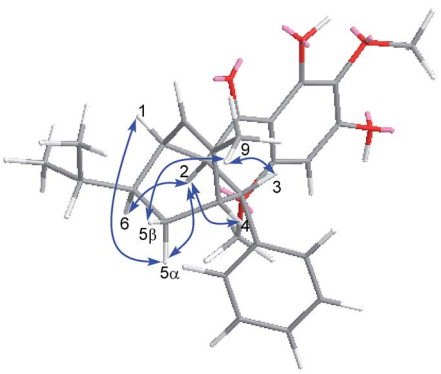

Fig. 4 Key ROESY correlations (blue arrows) of (−)-Celosine.

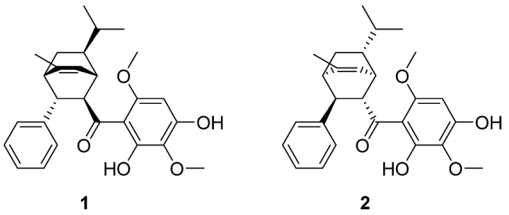

Fig. 5 The two possible configurations of (−)-Celosine.

Based on the skeleton of Celosine, Diels–Alder cycloaddition[8–15] would be the best choice to complete the total synthesis (Scheme 1). Diene compound **3** (or compound **4**) and dienophile compound **5**,[16] which was also isolated from *Celosia cristata* L. and other CTMs,[17,18] are the two key intermediates to construct Celosine **1** (or Celosine **2**) through asymmetric endo Diels–Alder cycloaddition. α-Phellandrene, named after *Eucalyptus phellandra*, is also a natural product,[18] and the only commercial available isomer (−)-α-phellandrene (diene compound **4**) was used for the synthesis of Celosine **2**. Compound **5** could be generated through Friedel Crafts acylation reaction from 2,5-dimethoxybenzene-1,3-diol (compound **6**) and cinnamoyl acid or chloride (compound **7** or **8**).

After preparation of the key intermediate **5** (ESI S7†), attention was turned to the asymmetric Diels–Alder cycloaddition. Huan and his coworkers[19] published a robust Diels–Alder cycloaddition method *via* the catalysis of silver nanoparticles supported by silica. As listed in Table 2, the reaction parameters shown in entry 1 and entry 2 are totally the same with Huan's, but the reaction results could not be accepted even though some product could be detected. From Huan's another paper,[20] we learned that the cycloaddition reaction was affected severely by the substituent groups on dienes and dienophiles. But we found that the multi-substituent groups on (−)-α-phellandrene (diene, compound **4**) and chalcone (compound **5**) made some obstacles for cycloaddition, and therefore, dichloroethane (DCE) was chosen for a higher reaction temperature. As shown in entry 4 and 5, the yields increased to 75% at 70 °C for 16 h after the change of solvent. What interests us most is that the cycloaddition could occur without participate of any catalyst as shown in entry 6 and 7 and only one regioisomer was detected, suggesting that the configuration of compound **2** was the most stable one based on thermodynamic theory.

The ^{1}H- and ^{13}C-NMR spectra showed that the natural source Celosine and the synthesized Celosine possessed the same 2D

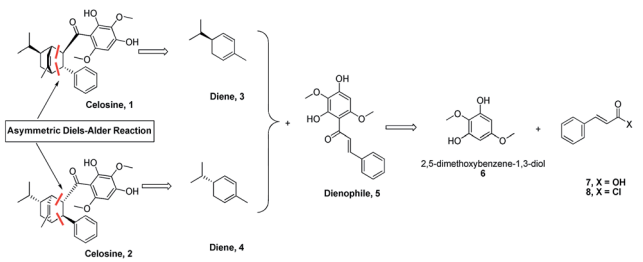

Scheme 1 Retro synthesis analysis of Celosine.

Table 2 Optimization of asymmetric Diels–Alder cycloaddition condition

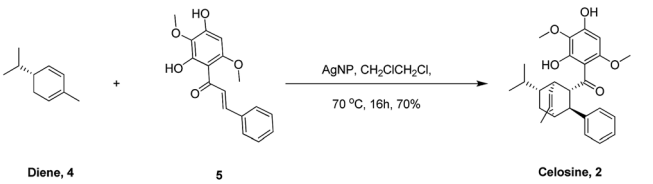

Entry	Catalyst	Solvent	Temp (°C)	Time (h)	Yield (%)	Endo/exo
1	AgNP[a]	DCM	25	16	10[b]	ND[c]
2	AgNP	DCM	40	16	25–30	ND
3	AgNP	DCE	40	16	20–25	ND
4	AgNP	DCE	50	16	50	Endo only[d]
5	AgNP	DCE	70	16	75	Endo only
6	—[e]	DCE	70	16	15	ND
7	—	DCE	70	48	45	Endo only

[a] Silver nanoparticles. [b] TLC semi quantitive. [c] Not detected. [d] Determined by chiral HPLC. [e] No catalyst.

structure (ESI S15†). However, the specific optical rotation ($[\alpha]_D^{25} = +142.6$ ($c = 0.1$, MeOH)) of the synthesized Celosine was opposite to that of the natural one, demonstrating that the structure of Celosine **1** was the exact structure of the natural Celosine. To further search the correlation between the two Celosines, CD spectroscopy was collected as depicted in Fig. 6. Totally opposite signals had been recorded either, confirming that the two compounds were enantiomers. Fortunately, the crystal structure of Celosine **2** was obtained and lead to a successful single crystal X-ray diffraction with anomalous dispersion of Cu Kα radiation (Fig. 7), which confirmed the planar structure and unambiguously determined the absolute configuration of Celosine **2**. As the mirror image of Celosine **2**, the planar structure and absolute configuration of Celosine **1** was also confirmed by comparing their CD data and the specific optical rotation data. Thus the natural source Celosine and the synthetic Celosine were renamed as (−)-Celosine and (+)-Celosine respectively based on their opposite specific optical rotation.

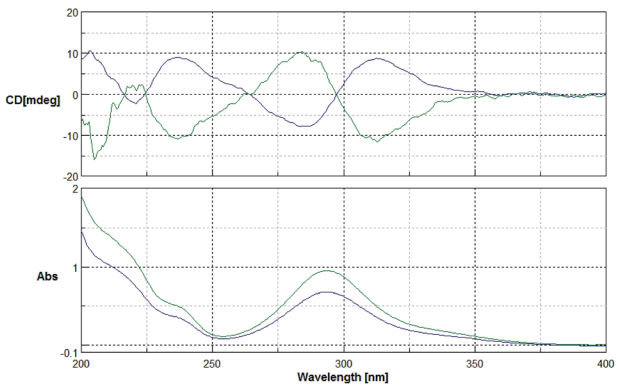

Fig. 6 CD spectrum of the two Celosines (green line for natural source Celosine, and the blue line for synthetic Celosine).

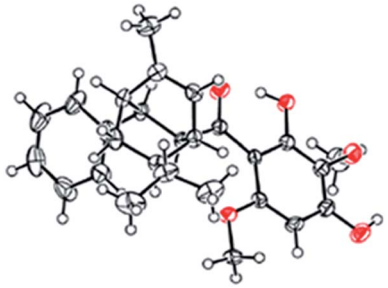

Fig. 7 The crystal structure of Celosine 2.

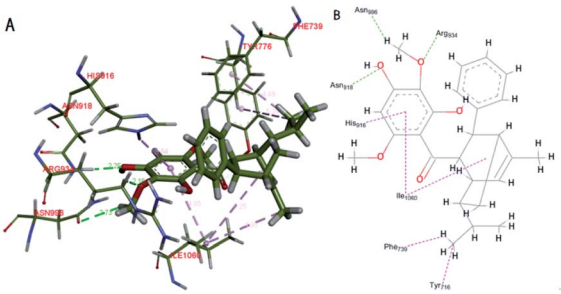

Fig. 8 Docking of (−)-Celosine into the binding site of MPO. Hydrogen bonds are shown as green dotted line. Hydrophobic bonds are shown as pink dotted line ((A) schematic perspective (B) plan sketch).

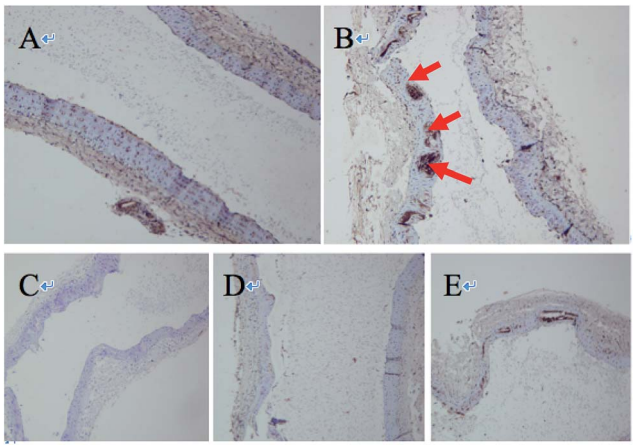

Fig. 9 Immunohistochemical picture of vascular protein MPO ((A) normal group, (B) disease group, (C) atorvastatin group, (D and E) (−)-Celosine high/low dose group).

Knowledge discovery in database (KDD) is a new information processing techniques quickly emerging in recent years with the aim to discover useful information hidden in databases currently available by making use of various information processing tools.[21–24] KDD was initially used in the field of TCM to predict the pharmacological target by searching DNP and MDDR3D databases. Myeloperoxidase (MPO), also known as peroxidase, is a heme protease with a heme prosthetic group. This leukocytic ferment mainly secreted by neutrophils plays an important role in the formation of atherosclerosis, and the increased expression and activity of MPO can promote the formation of atherosclerosis. As the classical target of anti-atherosclerosis, MPO was chosen as a predicted target for further study (ESI S17†).

Based on the docking study, the (−)-Celosine molecule could form multiple interactions with the residues around the docking pocket of MPO. MD simulation proved that the result of complex docking is stable and reliable (ESI S17†). The interaction between the (−)-Celosine molecule and important residues including HIE916, ASN918, ARG934, ASN996, TYR776, PHE739 and ILE1060 indicated the orientation of further optimization (Fig. 8). It was predicted by the KDD and MPO docking study that (−)-Celosine should possess an anti-atherosclerosis activity. To validate the prediction, (−)-Celosine was used to treat atherosclerosis in rat model established by feeding of high-fat diet and clamping of the carotid artery. The expression of MPO, MMP-9 and Lp-PLA2 was detected by using atorvastatin as the positive control.

As listed in Table 3, the expression of MPO and MMP-9 was increased significantly in modeled group and high dose (−)-Celosine treatment improved the vascular function of the carotid artery significantly in a dose dependent manner. However, no significant effect was observed on the expression of Lp-PLA2. HE staining showed significant atherosclerotic changes in the modeled group, as represented by endothelial detachment, rupture, intimal thickening and inward bulge, and obvious plaque formation. The degree of intimal thickening and uplift was greatly improved after (−)-Celosine treatment (ESI S22†). Immunohistochemistry showed high MPO expression in large number of endothelial cells in modeled group. In contrast, the MPO expression was decreased significantly in (−)-Celosine treatment group in a dose dependent manner (Fig. 9).

Table 3 Expression of MPO, MMP-9 and Lp-PLA2 in different animal groups

		MPO	MMP-9	Lp-PLA2
Norm group		11.19 ± 3.53	4.78 ± 0.36	19.98 ± 2.62
Disease group		19.69 ± 5.21[a]	9.22 ± 0.90[a]	22.17 ± 4.56
Atorvastatin group		16.62 ± 3.66	5.56 ± 0.33	21.76 ± 1.63
(−)-Celosine group	High dose	15.07 ± 2.98	5.73 ± 0.66	21.55 ± 1.01
	Low dose	15.36 ± 2.86	6.08 ± 0.28	21.91 ± 3.04

[a] $p > 0.05$.

Conclusions

In summary, (−)-Celosine with a new carbon skeleton, was isolated from *Celosia cristata* L., whose structure and relative configuration was confirmed by the spectroscopic and chemical methods. The total synthesis and the single crystal structure of the (+)-Celosine unfolded the true picture of the two compounds. Based on the KDD technique, (−)-Celosine was predicted as having an anti-atherosclerosis activity, and MPO, the classical target of anti-atherosclerosis, was chosen for docking and MD simulation study. MD simulation demonstrated that the result of complex docking was stable and reliable. The anti-atherosclerosis tests *in vivo* showed that the expression of MPO was decreased significantly after (−)-Celosine treatment, indicating the prediction was precise and rational. This finding has provided a new structure class for the treatment of atherosclerosis and related diseases.

Conflicts of interest

There are no conflicts to declare.

Acknowledgements

This work is supported by The seed fund program of Shanghai university of medicine & health Sciences (HSMF-17-22-031), Excellent Young Medical Expert of Shanghai (2017YQ048), China Postdoctoral Science Foundation (184279) and research project of Shanghai municipal health and Family Planning Commission (201540027), Shanghai Rising-Star Program (16QB1403800).

Notes and references

1 J.-J. Zhang, L.-Y. Xu and H. Shi, *Chin. J. Pharm.*, 2006, **15**, 25–26.
2 J.-F. Chen and Y. Yan, *Chin. J. Patho. Bio.*, 2010, **5**, 720–724.
3 D.-B. Weng, H.-F. Wang and J.-Y. Weng, *Chin. Bull. Bot.*, 2000, **17**, 565–568.
4 M. Begam, S. Narwal, S. Roy, S. Kumar, M.-L. Lodha and H.-C. Kapoor, *Biochemistry*, 2006, **71**, S44–S48.
5 J.-J. Wang, X.-M. Zhang and Z.-W. Huang, *Northwest Pharm. J.*, 2008, **06**, 354–356.
6 Y. Wang, Z.-Y. Lou, Q.-B. Wu and M.-L. Guo, *Fitoterapia*, 2010, **81**, 1246–1252.
7 X. Pang, H. X. Yan, Z.-F. Wang, M.-X. Fan, Y. Zhao, X.-T. Fu, C.-Q. Xiong, J. Zhang, B.-P. Ma and H.-Z. Guo, *J. Asian Nat. Prod. Res.*, 2014, **16**, 240–247.
8 C.-F. Chang, C.-F. Li, C.-C. Tsai and T.-H. Chuang, *Org. Lett.*, 2016, **18**, 638–641.
9 G. Yang, Q.-F. Jia, L. Chen, Z.-Y. Du and J. Wang, *Chem. inform.*, 2016, **47**, 76759–76763.
10 J. Zhang, Y.-L. Xiao, K. Chen, W.-Q. Wu, H.-F. Jiang and S.-F. Zhu, *Adv. Synth. Catal.*, 2016, **358**, 2684–2691.
11 A.-C. Aragonès, N.-L. Haworth, N. Darwish, S. Ciampi, N.-J. Bloomfield, G.-G. Wallace and I. Diez-Perez, *Nature*, 2016, **531**, 88–91.
12 M.-J. Umerani, D.-J. Dibble, A.-G. Wardrip, A. Mazaheripour, E. Vargas, J.-W. Ziller and A.-A. Gorodetsky, *J. Mater. Chem. C*, 2016, **4**, 4060–4066.
13 J.-E. Sears and D.-L. Boger, *Acc. Chem. Res.*, 2016, **49**, 241–251.
14 S. Gupta, M.-I. Alam, T.-S. Khan, N. Sinha and M.-A. Haider, *RSC Adv.*, 2016, **6**, 60433–60445.
15 R. Huang, X. Chang, J. Li and C.-J. Wang, *J. Am. Chem. Soc.*, 2016, **138**, 3998–4001.
16 M. Ahmed, M. Khaleduzzaman and M.-S. Islam, *Phytochemistry*, 1990, **29**, 2009–2011.
17 Y. Hua, L. He and H.-Q. Wang, *China J. Chin. Mater. Med.*, 2003, **28**, 530–533.
18 Z.-L. Liu and S.-S. Du, *E-J. Chem.*, 2011, **8**, 1937–1943.
19 H. Cong, C.-F. Becker, S.-J. Elliott, M.-W. Grinstaff and J. A. Porco, *J. Am. Chem. Soc.*, 2010, **132**, 7514–7518.
20 H. Cong, D. Ledbetter, G.-T. Rowe, J.-P. Caradonna and J.-A. Porco, *J. Am. Chem. Soc.*, 2008, **130**, 9214–9215.
21 J.-S. Fang, A.-L. Liu and G.-H. Du, *Acta Pharmacol. Sin.*, 2014, **49**, 1357–1364.
22 M. Whittle, P. Willett, W. Klaffke and P. van Noort, *J. Chem. Inf. Comput. Sci.*, 2003, **43**, 449–457.
23 M. Xue, M.-Y. Zheng, B. Xiong, Y.-L. Li, H.-L. Jiang and J. K. Shen, *J. Chem. Inf. Model.*, 2010, **50**, 1378–1386.
24 E.-J. Gardiner and V.-J. Gillet, *J. Chem. Inf. Model.*, 2015, **55**, 1781–1803.